

# The Effect of LiFePO<sub>4</sub> Coating on Electrochemical Performance of LiMn<sub>2</sub>O<sub>4</sub> Cathode Material

*Sadeghi, Behzad; Sarraf-Mamoory, Rasoul\*<sup>+</sup>; Shahverdi, Hamid Reza*

*Department of Materials Engineering, Tarbiat Modares University, P.O. Box 4838-141 Tehran, I.R. IRAN*

**ABSTRACT:** *LiMn<sub>2</sub>O<sub>4</sub> spinel cathode materials have been successfully synthesized by solid-state reaction. Surface of these particles were modified by nanostructured LiFePO<sub>4</sub> via sol gel dip coating method. Synthesized products were characterized by thermally analyzed by Thermogravimetric and Differential Thermal Analysis(TG/DTA), X-Ray Diffraction (XRD), Scanning Electron Microscopy (SEM), and Energy Dispersive X-ray (EDX) spectroscopy. The results of electrochemical tests showed that the charge/discharge capacities improved up to 120 mAh/g and charge retention of battery enhanced over %95. This improved electrochemical performance is caused by LiFePO<sub>4</sub> phosphate layer on surfaces of LiMn<sub>2</sub>O<sub>4</sub> cathode particles.*

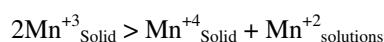
**KEY WORDS:** *Spinel, Solid state, Nanostructure, Sol gel dip coating, Phosphate.*

## INTRODUCTION

Since the birth of the lithium ion battery in the early 1990s, its development has been very fast and it has been widely applied as power source for a lot of light and high value electronics due to its significant advantages over traditional rechargeable battery systems[1,2]. Due to its low cost and low toxicity, the spinel LiMn<sub>2</sub>O<sub>4</sub>, the cathode for Li-ion batteries, has been extensively investigated. The spinel LiMn<sub>2</sub>O<sub>4</sub> has a cubic structure with the space group of Fd3m symmetry in which lithium and manganese ions occupy tetrahedral (8a) sites and octahedral (16d) sites, respectively, within a cubic close-packed oxygen array with oxygen ions in 32e sites. Many reports revealed that the spinel LiMn<sub>2</sub>O<sub>4</sub> offers a potentially attractive alternative to the presently commercialized LiCoO<sub>2</sub>. However, a key problem prohibiting LiMn<sub>2</sub>O<sub>4</sub> from commercialization is its severe capacity and cycling performance fading during cycling [3, 4]. Several factors cause capacity fade of spinel LiMn<sub>2</sub>O<sub>4</sub>,

as it had been reported by some investigators [5-11].

1- Dissolution of Mn<sup>3+</sup>. At the end of discharge, the concentration of Mn<sup>3+</sup> arrives at its highest level. Meanwhile, after cycling or storage, the surface of LiMn<sub>2</sub>O<sub>4</sub> is rich in Mn<sup>3+</sup>, contrary to the bulk structure. The Mn<sup>3+</sup> at the surface may disproportionate according to the following reaction



then, Mn<sup>2+</sup> ions from this reaction, dissolve in the electrolyte solutions.

2- Jahn–Teller effect. At the end of discharge, the Jahn–Teller effect happening at first on the surface of some particles may expand into an overall composition of Li<sub>1+δ</sub> [Mn<sub>2</sub>] O<sub>4</sub>. Thermodynamically speaking, this system is not really at equilibrium. The phase transition from a cubic into a tetragonal symmetry is a first-order process. Even though this kind of distortion is small,

\* To whom correspondence should be addressed.

+ E-mail: rsarrafm@modares.ac.ir

1021-9986/12/4/29

6/\$/2.60

it is big enough to destroy the structure to form a tetragonal structure, which is low in symmetry and high in disorder.

3- In organic solvents, the highly de-lithiated particles are not stable at the end of discharge; viz. the high oxidation ability of  $Mn^{4+}$  will lead to a decomposition of the solvents.

Recent research demonstrated that the importance of surface structural features of electrode materials for their electrochemical performance so, an effective strategy, coating the spinel  $LiMn_2O_4$  with organic and inorganic compounds, has been investigated. Jiang et al. [12] coated  $LiMn_2O_4$  spinel with 2wt. %Li-M- $PO_4$  (M =Co,Ni,Mn) and improved the discharge test showed that the cycling and rate capacities the spinel  $LiMn_2O_4$  cathode materials.  $LiFePO_4$  due to its potentially low cost, environmental benignness, and the belief that it could have a major impact in electrochemical energy storage, is the subject of many researches.. Also, it can be a good candidate for improving electrochemical properties of conventional cathodes like  $LiMn_2O_4$ .

In this study, we coated the  $LiMn_2O_4$  cathode with nanostructured  $LiFePO_4$  layer. The modified  $LiMn_2O_4$  can be protected from Mn dissolution, as the  $LiFePO_4$  nanostructure is formed on the surface of the spinel  $LiMn_2O_4$  cathode. The cycling and rate capacity of  $LiMn_2O_4$  cathode materials were significantly enhanced by stabilizing the electrode surface with  $LiFePO_4$  nanostructure.

## EXPERIMENTAL SECTION

### Synthesis of $LiMn_2O_4$

Spinel  $LiMn_2O_4$  powder was prepared by a solid-state reaction. All starting materials for the synthesis of  $LiMn_2O_4$  were purchased from merck company. To prepare this spinel, first manganese oxide (II) and lithium hydroxide with molar ratio of 7:3 was mechanically mixed. To achieve a more homogenous mixture and lowering calcification time, the mixture was prepared using a planetary mill with higher power, ball to power ratio of 10:1, and rotation speed of 200 rpm. Milling was stopped after 15 min and the obtained powder was heated in an electrical tube furnace for 5 hours. The heating rate of the furnace was  $10\text{ }^\circ\text{C min}^{-1}$ . It must be mentioned that the other parameters of the mill was supposed as constant.

### Synthesis of $LiFePO_4$ particles and nanostructure layers

Sol-gel synthesis is a low temperature, wet chemical approach, which is often used for the preparation of metal oxides or especially thin film. Standard sol-gel synthesis involves the formation of a sol, i.e., a stable colloidal suspension of solid particles in a solvent, and the gelation of the sol to form a gel consisting of interconnected rigid skeleton with pores made of colloidal particles. The properties of the gel are determined by the particle size and cross-linking ratio. The gel can then be dried to form xerogel, which shows reduced volume. To obtain the final products, all liquids need to be removed from the surface of pores by a heat treatment carried out at elevated temperatures [13].

As x ray diffraction peaks of  $LiFePO_4$  thin film layers cannot be detected due to low weight percentage, first we synthesized phosphate powders by sol gel process in determined optimum synthesis condition. Stoichiometric amounts of lithium phosphate ( $Li_3PO_4$ , Aldrich 33,889-3) and phosphoric acid ( $H_3PO_4$ , Merck, 100563) were dissolved in 200 mL water by stirring for 60 min. separately, citrate iron (III) (Merck, S3657400 219 was dissolved in 300 mL of water by stirring for 60 min. This two solutions were mixed together and obtained a transparent gel which was dried at  $70\text{ }^\circ\text{C}$  for 30h at atmosphere of 99.999% Argon. After grinding with a mortar and pestle, the obtained materials were calcined for 1 h. Calcination temperature was measured using Thermogravimetry and Differential Thermal Analysis (TG/DTA) result of the dried gel. The heating rate was  $10\text{ }^\circ\text{C min}^{-1}$ . Same sol was used for sol gel dip coating of samples. Three layers of phosphate coat were applied with drawl speed of 10 mm/min, remaining time of 2 min and up speed of 2 mm/min. After each coating step, the sample was dried  $70\text{ }^\circ\text{C}$  for 30 h. Final coated samples were calcined at  $670\text{ }^\circ\text{C}$  for 1h. Reaction conditions used for preparing different sample of  $LiMn_2O_4$  electrodes and  $LiFePO_4$  sol were listed in Table 1.

### Structural and morphological characterization of synthesized $LiMn_2O_4$ powder and $LiFePO_4$ sol

The thermal decomposition behavior of the gel was examined with a thermo-gravimetric analyzer (TGA, Perkin Elmer, TAC 7/DX) under  $N_2$  flow. Structural analysis of the obtained products was carried out using

Table 1: Reaction condition for the preparation of  $\text{LiMn}_2\text{O}_4$  and  $\text{LiFePO}_4$  sol.

Reaction condition for the preparation of $\text{LiMn}_2\text{O}_4$ electrode					Reaction condition for the preparation of $\text{LiFePO}_4$ sol				
Material used	Mn:Li ratio	Sample	Reaction Temp( $^{\circ}\text{C}$ )	Reaction Time(hrs)	Li Precursor	Fe Precursor	P Precursor	Solvent	Molar Ratio
$\text{MnO}_2 + \text{LiOH}$	7:03	A	900	5	$\text{LiOH}\cdot\text{H}_2\text{O}$	$\text{C}_6\text{H}_5\text{FeO}_7\cdot 2\text{H}_2\text{O}$	$\text{H}_3\text{PO}_4$	Deionized Water	1:03:02
		B	800						
		C	500						
		D	200						

an XRD instrument (Philips Expert) with radiation source of  $\text{Cu-K}\alpha$ . The surface morphology and energy dispersive spectrometry (EDAX) of the coated particles were taken with a SEM (Philips XL30) microscope.

### Electrochemical measurements

Charge and discharge diagrams and cyclic performance were conducted using the AUTOLAB-302 machine. In order to produce  $\text{LiMn}_2\text{O}_4$  cathode with coated  $\text{LiFePO}_4$ , first synthesized  $\text{LiMn}_2\text{O}_4$  as well as carbon black and PTFE binder were mixed together with ratio of 85:15:5 and were placed in a nickel mesh as current collector. Then, using the dip coating method this mesh was placed in the  $\text{LiFePO}_4$  sol to contaminate the surface of materials in the mesh. At the end, the mesh was heated at optimum calcination temperature for 1 h in Ar atmosphere. For the negative electrode, the graphite as well as carbon black and PTFE binder were mixed together with ratio of 85:15:5 and were placed in a nickel mesh as current collector. The used electrolyte was a 1M solution of  $\text{LiClO}_4$  in EC: DMC (1:1 ratio by volume). Charge/discharge and cyclic voltammetry experiments were carried out in a two-electrode glass cell that was built for this purpose. It must be noted that the battery assemble as well as all electrochemical experiments were performed within the glove-box at the presence of Ar atmosphere.

### RESULTS AND DISCUSSION

Fig. 1 presents DTA and TG diagrams produced for  $\text{LiFePO}_4$  gel from sole-gel process. The figure exhibits three distinct weight loss zones. At the first step, a weight drop of 6.4 % was observed which is due to evaporation of the physically absorbed water and degradation of

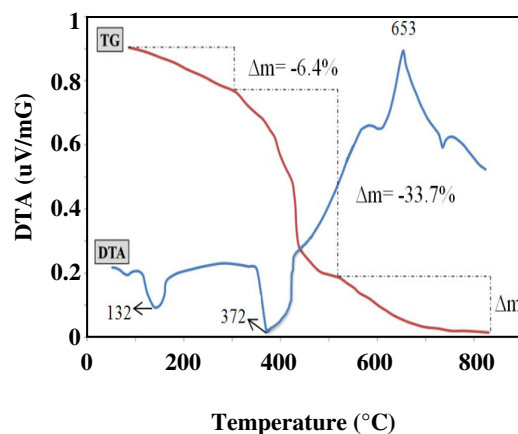


Fig. 1: TG and DTA diagrams of gel  $\text{LiFePO}_4$  at the range of room temperature to 850  $^{\circ}\text{C}$  in  $\text{N}_2$  atmosphere with heating rate of 10  $\text{mL}/\text{min}$ .

organic components with the sole. The second loss in within the temperature range of 200 to 500  $^{\circ}\text{C}$ , where weight drop is about 33.4 % which can be due to release of water during the crystallization as well as pyrolysis of citrate and other organic components. The last weight loss of the given gel will gradually initiate from the temperature of 522 $^{\circ}\text{C}$  and continue up to 800  $^{\circ}\text{C}$ . The weight drop in this zone is 11 % which is due to pyrolysis of remained organic components. All events during the heating of  $\text{LiFePO}_4$  gel in zones 1 and 2 took place at the temperatures of 132 and 372  $^{\circ}\text{C}$ , respectively. These reactions are endothermic while events occurred in zone 3 are at the temperature of 653  $^{\circ}\text{C}$  and are exothermic. So we selected the temperature 670  $^{\circ}\text{C}$  as calcination temperature.

Fig. 2 show the progression of the reaction between  $\text{MnO}_2$  and  $\text{LiOH}$  mixed in a 7:3 ratio from 200  $^{\circ}\text{C}$  to 900  $^{\circ}\text{C}$ .

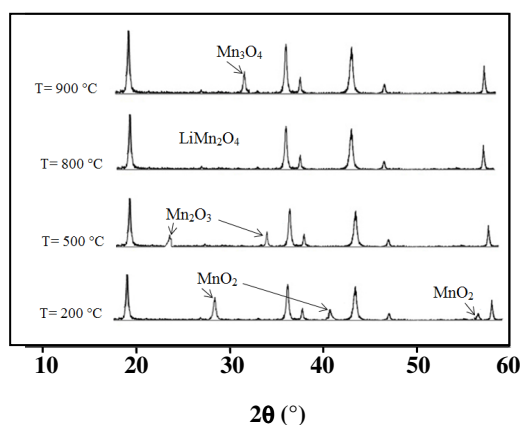


Fig. 2: Powder XRD patterns of  $\text{LiMn}_2\text{O}_4$  products after reaction at various temperatures.

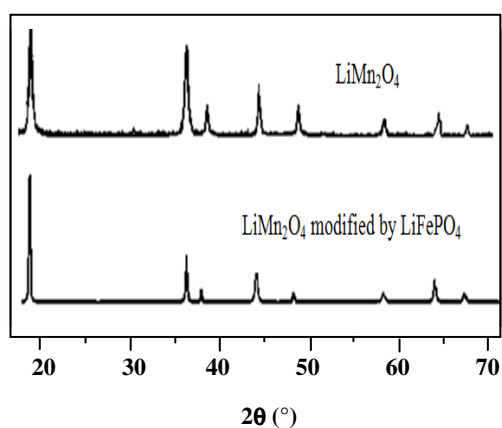


Fig. 3: XRD pattern of synthesized products uncoated bare  $\text{LiMn}_2\text{O}_4$ ,  $\text{LiMn}_2\text{O}_4$  coated with  $\text{LiFePO}_4$ .

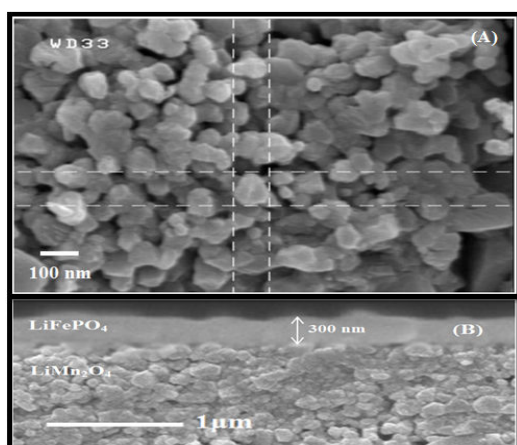


Fig. 4: SEM image (A) surface image (B) Cross-section image of  $\text{LiFePO}_4$  thin film deposited on  $\text{LiMn}_2\text{O}_4$  substrate.

As can be seen, the peaks of  $\text{LiMn}_2\text{O}_4$  without any impurities have been seen in 800 °C. Also,  $\text{MnO}_2$  and  $\text{Mn}_2\text{O}_3$  impurities can exist at 200 °C and 500 °C, respectively. The parameters like insufficient temperature and time, decomposition of unreacted  $\text{MnO}_2$ , can be reasons such impurities, respectively. On the other hand, the XRD patterns at 800 °C show clearly the characteristic peaks of the spinel  $\text{LiMn}_2\text{O}_4$  structure, e.g., the (111), (311), (222), (400), (331) and (511) peaks. When the heating temperature exceeds 800 °C, some characteristic peaks of  $\text{Mn}_3\text{O}_4$  appear due to excess manganese oxide present in original sample. Given these observations, it can be deduced that with increasing heating temperature, the crystallites of the spinel  $\text{LiMn}_2\text{O}_4$  grow and become ordered and at 800 °C a well-ordered spinel structure  $\text{LiMn}_2\text{O}_4$  is produced.

Fig. 3 displays XRD pattern for uncoated  $\text{LiMn}_2\text{O}_4$ , phosphate components of  $\text{LiFePO}_4$  and  $\text{LiMn}_2\text{O}_4$  coated by phosphate components of  $\text{LiFePO}_4$ . The lattice parameters of bare  $\text{LiMn}_2\text{O}_4$  and modified  $\text{LiMn}_2\text{O}_4$  were calculated from the XRD spectrum. They are 0.823 and 0.823 nm, respectively. The modified samples have a larger lattice constant than bare spinel, which indicated that  $\text{LiFePO}_4$  may form not only a thin layer on the surface of spinel but a solid solution by interacting with spinel. Fig. 4 shows the surface and cross-section SEM images of  $\text{LiFePO}_4$  thin film prepared by dip coating sol gel deposited on  $\text{LiMn}_2\text{O}_4$  substrate at 670 °C under argon atmosphere with the thickness of about 300 nm. As shown in Fig. 4, average grain size of about 100 nm. Fig. 4 shows the cross-section SEM image of  $\text{LiFePO}_4$  film with the thickness of about 300 nm, and it is a dense  $\text{LiFePO}_4$  film. Given this observation, we can conclude that  $\text{LiFePO}_4$  nanostructure film could form on  $\text{LiMn}_2\text{O}_4$  substrate.

Fig. 5 shows EDX analysis of the  $\text{LiFePO}_4$  nanostructure film. Each peak on the spectrum represents a transition with a characteristic energy. Every element has its own “fingerprint” of peaks so we can deduce which a represent. The P element can be clearly observed on the surface of modified materials.

The main difference of this study is applying nanostructured  $\text{LiFePO}_4$  coatings directly on cathode surface instead of surface of cathode particles. Fig. 6 shows the initial discharge profile with c-rate performances of the bare  $\text{LiMn}_2\text{O}_4$  and modified by  $\text{LiFePO}_4$  nanostructure

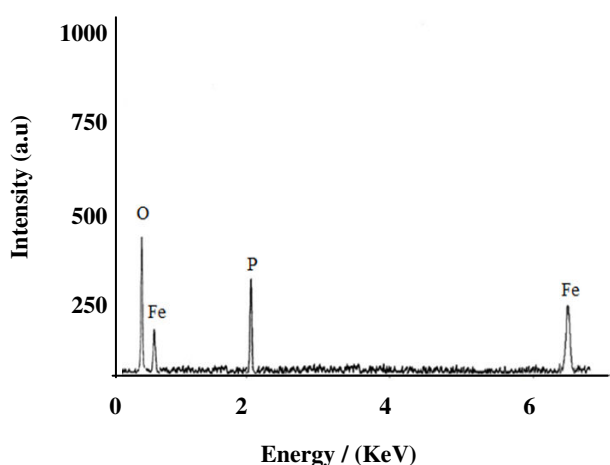


Fig. 5: EDX analysis of  $\text{LiFePO}_4$  nanostructure film.

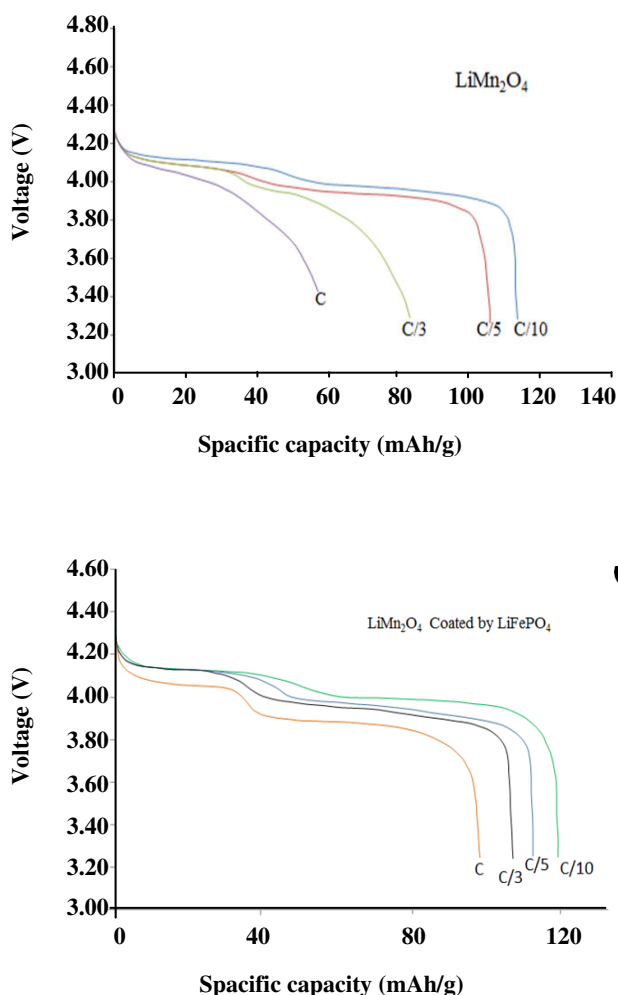


Fig. 6: Initial discharge capacities (A) bare  $\text{LiMn}_2\text{O}_4$  (B)  $\text{LiMn}_2\text{O}_4$  coated by  $\text{LiFePO}_4$ .

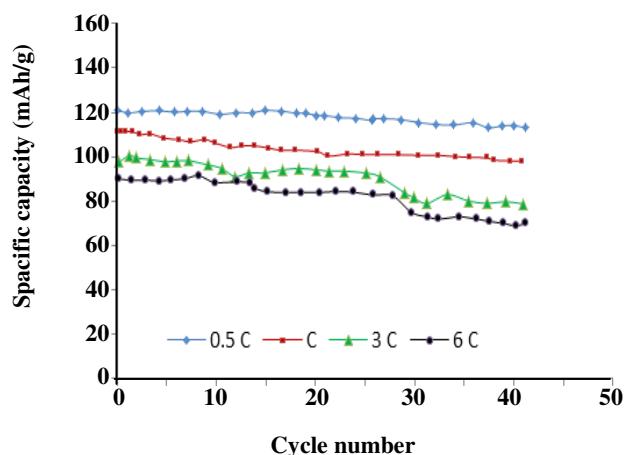


Fig. 7: Cycle properties of  $\text{LiMn}_2\text{O}_4$  modified by  $\text{LiFePO}_4$  nanostructure.

in the voltage range of 3.4 – 4.3 V. Two plateau feature of  $\text{LiMn}_2\text{O}_4$  can be seen in all curves which is the special characterization of Lithium manganese dioxide. Table 2 shows electrochemical characteristics of initial and coated  $\text{LiMn}_2\text{O}_4$  cathode samples. Maximum capacity drop is about 4.42% which occurred between 20th-40th cycles for the cathode materials coated by phosphate layers of  $\text{LiFePO}_4$ . These results would be ascribed to the increase of interfacial resistance due to coating layer on the surface of bare  $\text{LiMn}_2\text{O}_4$  material. Fig. 7 shows performance of the battery at higher speeds of discharge (higher powers). By increasing discharge speed, the drop of battery performance considerably decreases. Indeed, the amount of remained capacity to the initial capacity of the battery (120 mAh/g) with the rates of C/10, C/5, C/3, and C is 95%, 87.33%, 76%, and 71 %, respectively. It can be accepted that presence of  $\text{LiFePO}_4$  phosphate layer leads to a better electrical conductivity of the  $\text{LiMn}_2\text{O}_4$  particles as well as lowering or hindering the additional reactions of cathode materials with the electrolyte. All in all, this not only improves the cyclic capacity of the battery at the higher rates, but also results in higher discharge rates of cathode materials of  $\text{LiMn}_2\text{O}_4$  coated with phosphate layer of  $\text{LiFePO}_4$ .

## CONCLUSIONS

Effects on surface modification of the spinel  $\text{LiMn}_2\text{O}_4$  by a  $\text{LiFePO}_4$  nanostructure as a cathode for Li-ion batteries have been studied as an approach to investigate the

**Table 2: Electrochemical capacity and percent capacity retention bare  $\text{LiMn}_2\text{O}_4$  and  $\text{LiMn}_2\text{O}_4$  coated by  $\text{LiFePO}_4$ .**

Electrod composition	Initial discharge capacity(mAh/G)	40th discharge capacity (mAh/G)	Capacity retention (%) after 40th	Capacity loss between 20th-40th
$\text{LiMn}_2\text{O}_4$	118	90	69	22
$\text{LiMn}_2\text{O}_4$ Coated By $\text{LiFePO}_4$	120	113	95	4.42

electrochemical performance. The results of electrochemical tests showed better capacity retention due to coating layer on the surface of bare  $\text{LiMn}_2\text{O}_4$  material.

Received : Nov. 17, 2011 ; Accepted : Apr. 17, 2012

## REFERENCES

- [1] Fu L.J., Liu H., Li C., Wu Y.P., Rahm E., Holze R., Wu, H.Q., Surface Modification of Electrode Materials for Lithium Ion Batteries, *J. Solid State Sciences*, **8**, p. 113 (2006).
- [2] Lee C.W., Kim H.S., Moon S.I., Effects on Surface Modification of Spinel  $\text{LiMn}_2\text{O}_4$  Material for Lithium-Ion Batteries, *J. Materials Science and Engineering B*, **123**, p. 234 (2005).
- [3] Li X., Xu Y., Enhanced Cycling Performance of Spinel  $\text{LiMn}_2\text{O}_4$  Coated with  $\text{ZnMn}_2\text{O}_4$  Shell, *J. Solid State Electrochem*, **12**, p. 851 (2008).
- [4] Xia Y., Kumada N., Yoshio M., Enhancing the Elevated Temperature Performance of  $\text{LiLiMn}_2\text{O}_4$  Cells by Reducing  $\text{LiMn}_2\text{O}_4$  Surface Area, *J. Power Sources*, **90**, p. 135 (2000).
- [5] Gummow R.J., de Kock A., Thackeray M.M., Improved Capacity Retention in Rechargeable 4 V Lithium/Lithium-Manganese Oxide (Spinel) Cells, *J. Solid State Ionics*, **69**, p. 59 (1994).
- [6] Tarascon J.M., Coowar F., Amatucci G., Shokoohi F.K., Guy-omard D., Synthesis Conditions and Oxygen Stoichiometry Effects on Li Insertion Into the Spinel  $\text{LiMn}_2\text{O}_4$ , *J. Electrochem. Soc.*, **141**, p. 1421 (1994).
- [7] Yi T.F., Zhu Y.R., Zhu X.D., Shu J., Yue C.B., Zhou A.N., A Review of Recent Developments in the Surface Modification of  $\text{LiMn}_2\text{O}_4$  as Cathode Material of Power Lithium-Ion Battery, *J. Ionics*, **15**, p. 779 (2009).
- [8] Kannan A.M., Manthiram A., Surface/Chemically Modified  $\text{LiMn}_2\text{O}_4$  Cathodes for Lithium-Ion Batteries, *Electrochem. Solid-State Lett.*, **5**, p. 167 (2002).
- [9] Ein E., Urian, R. Wen W., Mukerjee S., Low Temperature Performance of Copper/Nickel Modified  $\text{LiMn}_2\text{O}_4$  Spinels, *J. Electrochim Acta*, **50**, p. 1931 (2005).
- [10] Jang D., Shin, Y. Oh S., Dissolution of Spinel Oxides and Capacity Losses in 4V $\text{Li}/\text{Li}_x\text{Mn}_2\text{O}_4$  Cells, *J. Electrochem Soc.*, **143**, p. 2204 (1996).
- [11] Park Y.J., Kim J.G., Kim M.K., Kim H.G., Chung H.T., Park Y., Electrochemical Properties of  $\text{LiMn}_2\text{O}_4$  Thin Films: Suggestion of Factors for Excellent Recharge Ability, *J. Power Sources*, **87**, p. 69 (2000).
- [12] Jiang Q.L., Du K., Cao Y.B., Peng Z.D., Hu G.R., Liu Y.X., Synthesis and Characterization of Phosphate-Modified  $\text{LiMn}_2\text{O}_4$  Cathode Materials for Li-Ion Battery, *J. Chinese Chemical Letter*, **1551**, p. 5 (2010).
- [13] Toprakci O., Toprakci H. A.K., Ji L., Zhang X., Fabrication and Electrochemical Characteristics of  $\text{LiFePO}_4$  Powders for Lithium-Ion Batteries, *J. KONA Powder and Particle Journal*, **28**, p. 50 (2010).